The Journal of Antibiotics
https://doi.org/10.1038/s41429-026-00901-7

Japan Antibiotics Research Association
The Society for Actinomycetes Japan

ARTICLE

Repurposing Tirazone as an effective quorum-sensing inhibitor against *Pseudomonas aeruginosa* virulence and biofilm formation

Mengna Feng[1] · Xiaoyu Wu[2] · Xin Hu[1] · Yi Wu[1] · Shiyi Gou[1] · Qiman Ran[1] · Yang Yuan[1] · Ting Huang[1] · Lufeng Dan[1] · Yiwen Chu[1] · Xikun Zhou[3] · Kelei Zhao[1] · Lianming Du[1,4]

Received: 27 October 2025 / Revised: 7 January 2026 / Accepted: 21 January 2026

Abstract

Antibiotic resistance has emerged as a critical global public health challenge. Quorum sensing (QS), a density-dependent regulatory mechanism, plays a pivotal role in bacterial pathogenesis by coordinating virulence factor expression, making it a critical target for antivirulence therapy. Leveraging a drug repositioning strategy, this study investigated the antivirulence potential of drugs in the database of DrugBank on the common opportunistic pathogen *Pseudomonas aeruginosa* by virtual screening. Molecular docking analysis predicted that the antitumor drug, Tirazone, could bind to the core QS regulatory proteins, LasR, RhlR, and PqsR of *P. aeruginosa* with abundant active sites, whereas the binding free energies were higher than those of the native QS signals. In vitro experiments demonstrated that Tirazone significantly suppressed virulence factor secretion, cell motilities, and biofilm formation in the model *P. aeruginosa* strain PAO1, and downregulated the expression of a series of QS-related genes with low effective concentration (≤ 8 μM). A competitive binding model of QS signal molecules further elucidated that Tirazone interfered with QS signaling by competitively inhibiting the function of LasR, RhlR, and PqsR. Additionally, Tirazone treatment significantly protected *Caenorhabditis elegans* and mouse models from *P. aeruginosa* infection, and reduced the bacterial loads and pathological lesions in mouse lungs. Moreover, Tirazone demonstrated synergistic effects with polymyxin B, levofloxacin, and amikacin, significantly enhancing their bactericidal efficacy in treating *P. aeruginosa*. This study reveals the molecular mechanism underlying Tirazone's multi-target intervention in the QS system, and provides an experimental foundation for developing combination therapies based on antivirulence strategies.

Introduction

The discovery of penicillin in 1928 ushered in a golden age of natural-product antibiotic research that peaked in the mid-1950s [1]. Nearly a century after the discovery of antibiotics, the antibiotic resistance crisis has become a major global public health challenge [2]. According to the World Health Organization (WHO), approximately 1.27 million people died directly from drug-resistant infections worldwide in 2019, and such deaths are expected to climb to 10 million per year by 2050 [3]. Although antibiotics have won critical victories against bacterial infections, resistance mechanisms that continue to evolve in pathogens are undermining the effectiveness of existing treatments. New antibiotic development faces a double dilemma: the discovery rate of innovative drugs continues to decline, while the efficacy of traditional antibiotics continues to decline, and the cost and technology threshold for new drug development have increased significantly [4]. Overcoming

These authors contributed equally: Mengna Feng, Xiaoyu Wu

Supplementary information The online version contains supplementary material available at https://doi.org/10.1038/s41429-026-00901-7.

✉ Kelei Zhao
zhaokelei@cdu.edu.cn

✉ Lianming Du
dulianming@cdu.edu.cn

[1] Antibiotics Innovation and Resistance Control Key Laboratory of Sichuan Province, School of Pharmacy, Chengdu University, Chengdu, China

[2] School of Electric Engineering, Xi'an Jiaotong University, Xi'an, China

[3] Department of Biotherapy, Cancer Center and State Key Laboratory of Biotherapy, West China Hospital, Sichuan University, Chengdu, China

[4] Institute for Advanced Study, Chengdu University, Chengdu, China

this crisis requires transcending traditional patterns and building new pathogen control systems through innovative strategies [5].

Quorum sensing (QS) is a bacterial cell-to-cell communication mechanism mediated by diffusible signal molecules known as autoinducers [6]. The core function of this system is to dynamically regulate gene transcription by sensing population density: maintaining covert colonization at low density, and simultaneously activating virulence factor expression and promoting biofilm formation at high density, thus breaking through host defenses [7]. QS inhibitors (QSIs) disrupt bacterial communication by degrading autoinducers or blocking receptor binding, effectively inhibiting pathogenicity and reducing resistance selection pressure. For example, farnesol and hamamelis may significantly enhance the efficacy of beta-lactams by increasing the susceptibility of *Staphylococcus aureus* to antimicrobial agents [8]. Recent studies further confirm that QSIs have important applications in inhibiting biofilm formation and attenuating pathogen virulence [9].

Pseudomonas aeruginosa is a Gram-negative opportunistic pathogen that accounts for approximately 10%-11% of nosocomial infections and can infect cystic fibrosis, burns, immunodeficiency, chronic obstructive pulmonary disease, cancer, and critically ill patients, such as COVID-19 mechanically ventilated patients [10]. This pathogen causes disease synergistically through multiple mechanisms: host colonization, motility regulation, biofilm formation, secretion of destructive enzymes, release of toxic secondary metabolites, and siderophore-mediated iron uptake systems [11]. The expression of virulence effectors is finely regulated by the QS system, which consists of three core pathways [12]: Las, Rhl, and Pqs. The Las system uses 3-oxo-C12-homoserine lactone (3-oxo-C12-HSL) (Fig. 1a) as a signal molecule, activates virulence factors such as elastase (LasB) and exotoxin A through the LasR transcription factor, and activates the downstream Rhl system [13]. The Rhl system relies on C4-HSL (Fig. 1b) to regulate rhamnolipid synthesis, pyocyanin production, and biofilm formation [14]. The Pqs system uses 2-heptyl-3-hydroxy-4 (1*H*)-quinolone (PQS) (Fig. 1c) to coordinate siderophore synthesis and stress response, and forms a cascade regulatory network with the Las/Rhl system [15]. Antibiotic resistance in this strain results from multiple mechanisms: reduced cell membrane permeability, gene expression of multidrug efflux pumps, antibiotic-inactivating enzyme production, and adaptive mutations and horizontal gene transfer in chronic infections [5]. These characteristics make it a challenging pathogen for clinical anti-infective therapy.

In this study, 20 candidate compounds were virtually screened from the DrugBank database by molecular docking technology, and the anti-QS activity of the anti-cancer drug Tirazone on *P. aeruginosa* was further explored by multi-dimensional experiments, including the production of extracellular proteases, pyocyanin, and rhamnolipids, biofilm formation, motility ability, the expression changes of QS-related genes, and the synergistic effect with antibiotics. The targeting of Tirazone on *P. aeruginosa* QS system was determined by using interaction simulation models followed by native QS signals and signal-negative strains-based competitive assay. Finally, the in vivo protection efficiency of Tirazone against *P. aeruginosa* infection was verified by using *Caenorhabditis elegans* and mouse models.

Materials and methods

Bacterial strains, media, and chemicals

The model *P. aeruginosa* strains PAO1 and PA14, QS signal-deficient strains PAO1-Δ*lasI*, PAO1-Δ*rhlI*, and PAO1-Δ*pqsA*, 8 clinical strains from patients with chronic obstructive pulmonary disease, and uracil auxotrophic *Escherichia coli* OP50 were kept in our laboratory [16]. The media used were Lysogeny Broth (LB), Mueller-Hinton broth (MH), M9-adenosine medium (0.1%, w/v), M9 skim milk medium [17], swimming agar medium (0.3%, w/v), swarming medium [18] (0.5% agar, 0.5% peptone, 0.2% Angel yeast powder, 1% glucose), twitching agar medium (1%, w/v), peptone-glucose sorbitol agar medium (PGS) [17], and *P. aeruginosa* selective medium. The compounds Tirazone, 3-oxo-C12-HSL, C4-HSL, and PQS were purchased from MedChemExpress Co. Ltd. (Shanghai, China) with a purity of ≥ 98%, dissolved in DMSO according to instructions, and diluted to a working concentration of 100 mM for further use. Tribromoethanol (Avertin®, Sigma-Aldrich T48402) was purchased from Sigma-Aldrich (Shanghai) Trading Co., Ltd. and freshly prepared in PBS to 25 mg/mL. A single colony of *P. aeruginosa* PAO1 was picked and cultured overnight at 37 °C in LB broth with shaking (180 rpm), and then the absorbance value of cell density at 600 nm (OD_{600}) was adjusted to 1.0 with sterile physiological saline for standby.

Molecular docking

The software Dockey was used to analyze the interaction between candidate compounds (Table S1) and the three key QS regulatory proteins of *P. aeruginosa* [19]. The 3D molecular structure of Tirazone was obtained from PubChem database and stored in standard SDF format; then the crystal structure files of LasR (ID: 3IX3), RhlR (ID: P54292) and PqsR (ID: 6B8A) were downloaded from PDB database and stored in PDB format respectively for subsequent molecular docking. The molecular docking results were analyzed by PyMOL and Discovery Studio.

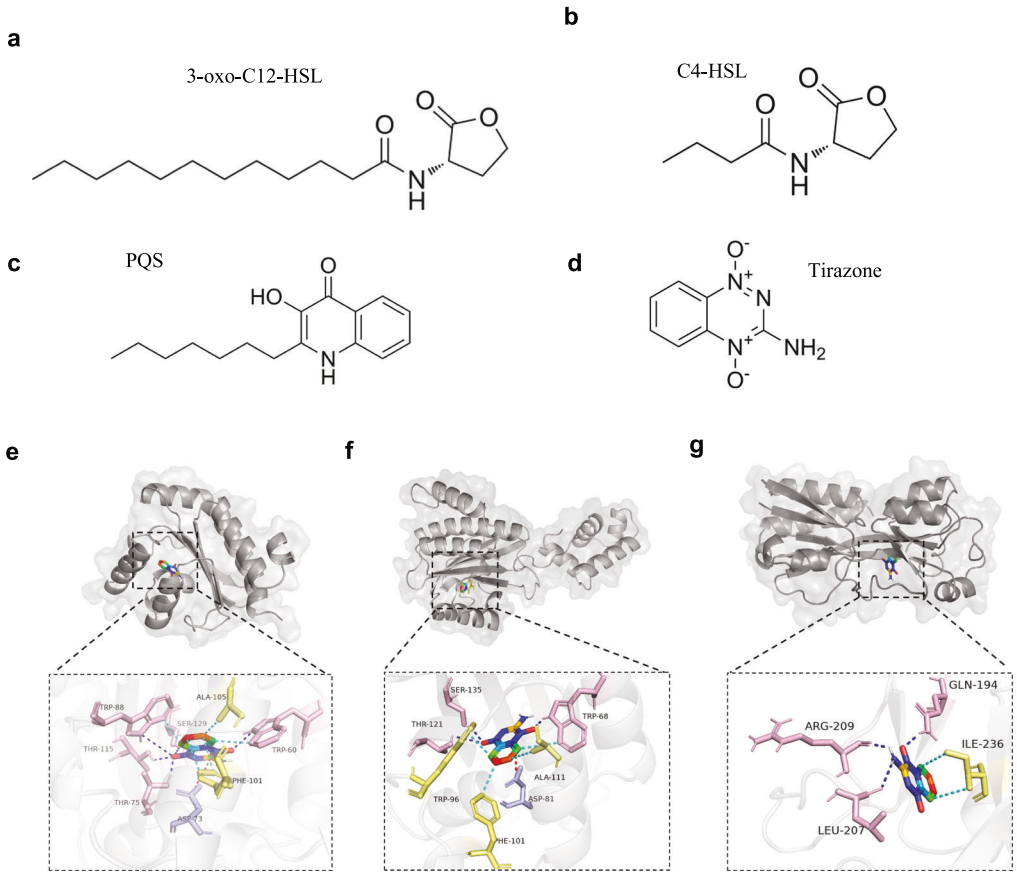

h

Rcepters	Ligands	Docking scores (kcal/mol)	H-bonds	hydrophobic interaction	π-stacking
LasR	3-oxo-C12-HSL	-6.26	Tyr-64,**Thr-115**,**Ser-129**	Leu-40,**Tyr-64**,Tyr-56,Leu-125,Tyr-47,Leu-36,Ala-127,Ala-50	
	Tirazone	-5.48	Trp-60,Trp-88,Thr-75,**Thr-115**,**Ser-129**	Trp-60,Trp-88,Phe-101,Ala-105	Asp-73
RhlR	C4-HSL	-5.14	**Trp-68**,**Ser-135**,Tyr-64,**Asp-81**	Tyr-72,**Trp-96**,Trp-68,Ile-84,Leu-107	/
	Tirazone	-4.43	**Trp-68**,**Ser-135**,Thr-121	Trp-68,Phe-101,**Trp-96**,Ala-111	Asp-81
PqsR	PQS	-6.88	Gln-194,Arg-209	Leu-197,Phe-221,**Ile-236**,Ile-149	/
	Tirazone	-4.88	**Gln-194**,**Arg-209**,Leu-207	**Ile-236**	/

Fig. 1 Molecular docking validation of Tirazone with PqsR (PDB ID:6B8A), LasR (PDB ID:3IX3) and RhlR(PDB ID:P54292). **a** QS signal molecule 3-oxo-C12-HSL. **b** QS signal molecule C4-HSL. **c** QS signal molecule PQS. **d** Tirazone. **e** Three-dimensional structure of Tirazone-LasR docking. **f** Three-dimensional structure of Tirazone-RhlR docking. **g** Three-dimensional structure of Tirazone-PqsR docking, π- stacking interaction (red) and hydrogen bonds (dark blue). **h** Docking scores and binding sites of receptors with ligands

Susceptibility testing

The minimum inhibitory concentration (MIC) of candidate compounds against *P. aeruginosa* PAO1 was determined using the broth dilution method [20]. Briefly, 1×10^5 CFU/mL of *P. aeruginosa* PAO1 was cultured in 100 μL of MH broth containing different concentrations of test compounds, and then incubated at 37 °C for 18–20 h, followed by absorbance measurement at 600 nm. All the experiments were independently repeated at least three times.

In vitro screening

The growth of *P. aeruginosa* PAO1 in M9 minimal medium supplemented with adenosine as the sole carbon source was monitored to preliminarily test its QS ability [21]. Briefly, *P. aeruginosa* PAO1 with $OD_{600} = 1.0$ was added at 1:100 to 200 μL of M9 adenosine medium (0.1%, w/v), which contained different concentrations of the test compound (Table S1), aliquoted into 96 wells, and incubated at 37 °C for 36 h followed by absorbance measurement at 600 nm. All the experiments were independently repeated at least three times.

Extracellular protease production activity of *P. aeruginosa* was determined by its proteolytic capacity [22]. A total of 2 μL of *P. aeruginosa* PAO1 solution with $OD_{600} = 1.0$ was inoculated on the surface of M9 skim milk medium containing different concentrations of the test compound and cultured at 37 °C, and then the proteolytic ring diameter around the colony was measured after 14–16 h. All the experiments were independently repeated at least three times.

Chloroform extraction coupled with spectrophotometry was employed to determine the pyocyanin production in *P. aeruginosa* strains [23]. *P. aeruginosa* PAO1 or clinical isolates were inoculated into LB medium at a ratio of 1:100, and different volumes of Tirazone were added to make final concentrations of 1 μM, 2 μM, 4 μM, and 8 μM, respectively. Incubate at 37 °C, 180 rpm for 24 h, centrifuge for 5 min, add chloroform to the supernatant at a ratio of 5:3, separate layers, and then add 0.2 N HCl to the lower layer at a ratio of 3:1, shake vigorously. After stratification, 100 μL of supernatant was pipetted into 96-well plates and pyocyanin levels were quantified at 520 nm using a microplate reader. All the experiments were independently repeated at least three times.

The rhamnolipid production by *P. aeruginosa* was determined using the methylene blue colorimetric method [24]. *P. aeruginosa* PAO1 was inoculated into LB medium at a ratio of 1:100, and different volumes of Tirazone were added to make final concentrations of 1 μM, 2 μM, 4 μM, and 8 μM, respectively. Incubate at 37 °C, 180 rpm for 24 h, centrifuge for 5 min, collect supernatant, mix with an equal amount of ethyl acetate, shake vigorously, collect organic phase, dissolve in 4 mL chloroform, add 200 μL freshly prepared methylene blue solution (1 g/L, pH 8.6), and quantitatively determine at 638 nm. All the experiments were independently repeated three times.

Biofilm formation

Biofilm formation was quantified using the crystal violet staining assay [25]. *P. aeruginosa* PAO1 was inoculated 1:100 into LB medium supplemented with different volumes of Tirazone, aliquoted at 200 μL into 96-well plates, and incubated for 24 h. DMSO was added to the control group at the same volume, after which the bacterial culture suspension was removed and washed twice with PBS. The 96-well plate was dried in an oven and stained with 1% (w/v) CV for 30 min. The floating color was washed with PBS and dried, and 220 μL of 95% ethanol was added to dissolve the biofilm attached to the well wall, and then quantified at 595 nm. All the experiments were independently repeated at least three times.

Motility assay

The cell motilities of *P. aeruginosa* were assessed in semi-solid agar assays to test the swimming (0.3% agar), swarming (0.5% agar), and twitching motilities (1% agar) [26, 27]. Briefly, different volumes of Tirazone were added to swimming, swarming, and twitching media to make the final concentrations of 1 μM, 2 μM, 4 μM, and 8 μM, respectively. The media were left to solidify at room temperature for 24 h. The control group was added with the same amount of DMSO. Inoculate 2 μL of *P. aeruginosa* PAO1 solution in the middle, surface, and bottom of agar medium, place the medium plate in a constant temperature incubator at 37 °C overnight, and then measure the diameter of the range of motion. All the experiments were independently repeated at least three times.

Real-time quantitative PCR amplification (RT-qPCR)

RT-qPCR was used to analyze the regulatory effect of Tirazone on the expression of virulence genes of *P. aeruginosa* PAO1. The total RNA of Tirazone-treated *P. aeruginosa* PAO1 was isolated by using a bacterial RNA isolation kit, followed by genomic DNA removal and cDNA synthesis (Foregene Biotechnology Co. Ltd., China). SYBR Green fluorescent dye was used for RT-qPCR. The 16S rRNA gene was selected as the internal reference for normalizing gene expression levels, as it exhibits stable expression under our experimental conditions and is widely validated in related *P. aeruginosa* virulence research [17, 28, 29]. QS-related virulence genes of PAO1 include

lasB, *lasR*, *rhlA*, *rhlR*, *pqsA*, *pqsR*, *phzA1* and *hcnA* (Table S2). The relative expression level of the target gene was calculated by the $2^{-\Delta\Delta Ct}$ method [22], where $\Delta\Delta Ct = \Delta Ct_{sample} - \Delta Ct_{mean(DMSO)}$. All the experiments were independently repeated at least three times.

Target verification

The expression changes of QS-controlled genes (*lasB*, *rhlA*, *phzA1*) in signal-deficient strains (PAO1-Δ*lasI*, PAO1-Δ*rhlI*, PAO1-Δ*pqsA*) exposed to exogenous signal molecules (50 μM) and compound treatment were determined by RT-qPCR [28]. Briefly, the strains were cultured in LB medium supplemented with different combinations of native QS signal molecules (50 μM) and Tirazone (8 μM). The expression levels of *lasB*, *rhlA*, and *phzA1* genes regulated by QS were detected by RT-qPCR. Moreover, *P. aeruginosa* clinical isolates were cultured in M9-adenosine and LB medium supplemented with different combinations of native QS signal molecules (50 μM) and Tirazone (8 μM), followed by cell density determination and pyocyanin production measurement. All the experiments were independently repeated at least three times.

Tirazone-antibiotics combination test

Antibiotic-Tirazone synergy was assessed based on a checkerboard combination susceptibility test [30]: PAO1 solution with $OD_{600} = 1.0$ was inoculated into MH medium and diluted to 1×10^5 CFU/mL. Tirazone and gradient antibiotics were added at final concentrations of 1 μM, 2 μM, 4 μM, and 8 μM, respectively. OD_{600} absorbance was measured after incubation at 37 °C for 18 h. Amikacin-resistant (R4-1-12), polymyxin B-resistant (2-R2-6), and levofloxacin-resistant (3-R5-1) clinical isolates were tested simultaneously, and each group of experiments was repeated three times. Synergistic effects were quantified by the Bliss independence model [31] (formula: $S = f_{X,0} \cdot f_{0,Y} - f_{X,Y}$, where $S = 0$ indicates independent effects, $S > 0$ indicates synergy, and $S < 0$ indicates antagonism).

Caenorhabditis elegans model

The fast-killing assay was used to test the protection activity of Tirazone on *C. elegans* against *P. aeruginosa* challenge on PGS agar medium [32]. Briefly, 50 μL of *P. aeruginosa* PAO1 bacterial solution ($OD_{600} = 1.0$) was evenly spread on PGS plates containing 8 μM Tirazone or DMSO and cultured overnight at 37 °C. Subsequently, 10 adult nematodes at L4 stage (per group) were inoculated on *P. aeruginosa* PAO1 macrocolony and further cultured at 20 °C. The survival of nematodes was recorded every 8 h. The growth of nematodes on *E. coli* OP50 was set as the negative control. The experiment was independently repeated three times.

Mouse model

The acute lung infection model of mice was established by sublingually instilling *P. aeruginosa* into C57BL/6 mice [17, 33]. A total of 108 mice were randomly used for the survival monitoring assay ($n = 36$, 6 mice per group) and pathological analysis ($n = 72$, 12 mice per group). All the mice were anesthetized by intraperitoneal injection of Avertin (250 mg/kg), and confirmed by loss of righting reflex within 2 min. Avertin solutions were freshly prepared and filtered through a 0.22 μm membrane to minimize peritoneal irritation. Lung infection was established by sublingual instillation of 30 μL of freshly prepared bacterial suspension (3.0×10^8 CFU/mL of PAO1 in saline) and 8 μM of Tirazone. Tirazone treatment (intraperitoneal injection) was repeated every 12 h post-infection. The survival of mice was recorded by observers blinded to the groups. For the pathological analysis assay, the randomly selected mice with acute lung infection caused by *P. aeruginosa* were killed at designated sampling points and the whole lungs were harvested. The left lobe was fixed in 4% paraformaldehyde for paraffin sectioning and hematoxylin-eosin (HE) staining. The remaining lung tissue (0.1–0.3 g) was washed with normal saline, mechanically homogenized, serially diluted, and then smeared on *P. aeruginosa* selective medium and cultured for 18 hours at 37 °C, followed by CFU enumeration.

Ethical statement

The C57BL/6 mice (8-week-old, female) were purchased from Huafukang Bioscience Co., Ltd. (Chengdu, China) and maintained under standard housing conditions (temperature of 20 °C to 24 °C, humidity of 50 to 60%) in the Specific Pathogen-Free (SPF) facility at the State Key Laboratory of Biotherapy, Sichuan University. All animal procedures were approved by the Ethics Committee of the State Key Laboratory of Biotherapy (2021559 A) and strictly followed the Institutional Guidelines for Animal Care and Use of Sichuan University.

Statistical analysis

All statistical analyses and graphs were performed using GraphPad Prism 9.0.1 (GraphPad Software, San Diego, CA, USA). Experimental data are expressed as Mean ± SD. The following methods were used for analysis of differences between groups, depending on the type of data: For comparisons among three or more groups, continuous data (such as bacterial burden) were analyzed by one-way ANOVA.

Bacterial colony-forming unit (CFU) counts were log10-transformed prior to ANOVA to satisfy the assumption of normality. If a significant difference was found by ANOVA ($P < 0.05$), it was followed by Dunnett's multiple comparisons test for comparisons versus the control group. For comparisons between two groups, an unpaired Student's t test was used. The Mantel-Cox log-rank test was used for survival analysis.

Results

Docking of Tirazone with QS receptors of *P. aeruginosa*

To investigate the molecular interactions between test compounds (Table S1) and key quorum-sensing (QS) target proteins in *P. aeruginosa*, systematic molecular docking analyses targeting LasR, RhlR, and PqsR were performed. Molecular docking simulations using Dockey software revealed distinct binding patterns of Tirazone (Fig. 1d) with these regulatory targets. Structural analysis through PyMOL identified specific hydrogen-bonding interactions between Tirazone and critical residues: Thr115/Ser129 in LasR, Trp68/Ser135 in RhlR, and Gln194/Arg209 in PqsR (Fig. 1e–h). Further binding-mode analysis with Discovery Studio demonstrated that although the absolute binding free energy of Tirazone to all three receptors was lower than that of their corresponding natural ligands (Fig. 1h), it could successfully dock into the ligand-binding pocket of each receptor (Fig. S4a–c). Notably, Tirazone exhibited differential stabilization mechanisms: in LasR and RhlR, its binding was stabilized by high-strength salt-bridge interactions (Figs. S1 and S2), whereas in PqsR, its core triazole ring showed significant shape complementarity with a unique hydrophobic pocket formed by residues Leu207, Gln194, and Arg209 (Figs. S3 and S4d). Collectively, these findings suggest that Tirazone may achieve synergistic targeting through a non-classical, multimodal mechanism that integrates selective hydrogen bonding, electrostatic interactions, and optimized hydrophobic packing. Collectively, these findings suggested that Tirazone might achieve target engagement through atypical binding mechanisms combining selective hydrogen bonding and optimized hydrophobic packing.

QS-mediated growth inhibition of *P. aeruginosa* by the candidate compounds

Antivirulence therapeutics represent a strategic approach to combat bacterial infections by selectively disrupting virulence factor production while avoiding bactericidal pressure that drives resistance development [34]. To specifically evaluate QS inhibitory activity, we used M9-adenosine minimal medium as a QS-dependent growth reporter system. *P. aeruginosa* lacks constitutive enzymes for adenosine metabolism; instead, its ability to utilize adenosine as a sole carbon source requires the expression of a nucleoside hydrolase (Nuh) strictly regulated by the Las QS system [21]. This design ensures that growth inhibition in M9-adenosine medium reflects specific interference with QS signaling, rather than non-specific metabolic toxicity. In contrast, LB medium is a nutrient-rich complex medium that supports growth independent of QS-dependent pathways, serving as a critical control to rule out general bacteriostatic effects. Initial screening tested the bactericidal activity of the 20 candidate compounds in MH broth and the preliminary QS inhibitory activity in the QS-required medium M9-adenosine. Finally, six compounds with no bactericidal activity, while significantly suppressed the growth of *P. aeruginosa* PAO1 in M9-adenosine were obtained (Table S1 and Fig. S5). Notably, Tirazone demonstrated potent species-wide efficacy, completely suppressing growth of PAO1, PA14 and clinical isolates at 8 μM in M9-adenosine medium (Figs. 2a and S6a). This inhibition proved adenosine metabolism-dependent, as equivalent Tirazone concentrations exerted no growth inhibitory effects in LB medium (Figs. 2b and S6b). Contrastingly, Benzophenone, Coumarin 120, Abametapir, Tricyclazole, and Cryptotanshinone showed partial or negligible activity under identical conditions (Fig. S5). The adenosine-dependent growth suppression pattern, coupled with preserved viability in LB medium, indicated that Tirazone might be used as a potential compound for developing QSIs.

Tirazone inhibits the QS-related phenotypes of *P. aeruginosa*

P. aeruginosa employs its QS network to coordinate the biosynthesis and secretion of virulence effectors such as extracellular proteases, pyocyanin, and rhamnolipids—pathogenicity determinants that induce host tissue necrosis and systemic organ failure [10]. To functionally explore QS-mediated virulence regulation, we first developed a model of nutrient limitation using M9-skim milk medium as the sole carbon source, in which QS activation prompted *P. aeruginosa* PAO1 to secrete extracellular proteases for substrate hydrolysis [35]. We subsequently screened six structurally diverse candidate compounds (Benzophenone, Coumarin 120, Abametapir, Tricyclazole, Cryptotanshinone, and Tirazone) (Table S3) for their abilities to disrupt QS-regulated extracellular protease secretion cascade. Dose-response analyses revealed that Tirazone exhibited significant concentration-dependent inhibition of protease secretion compared to the other five compounds

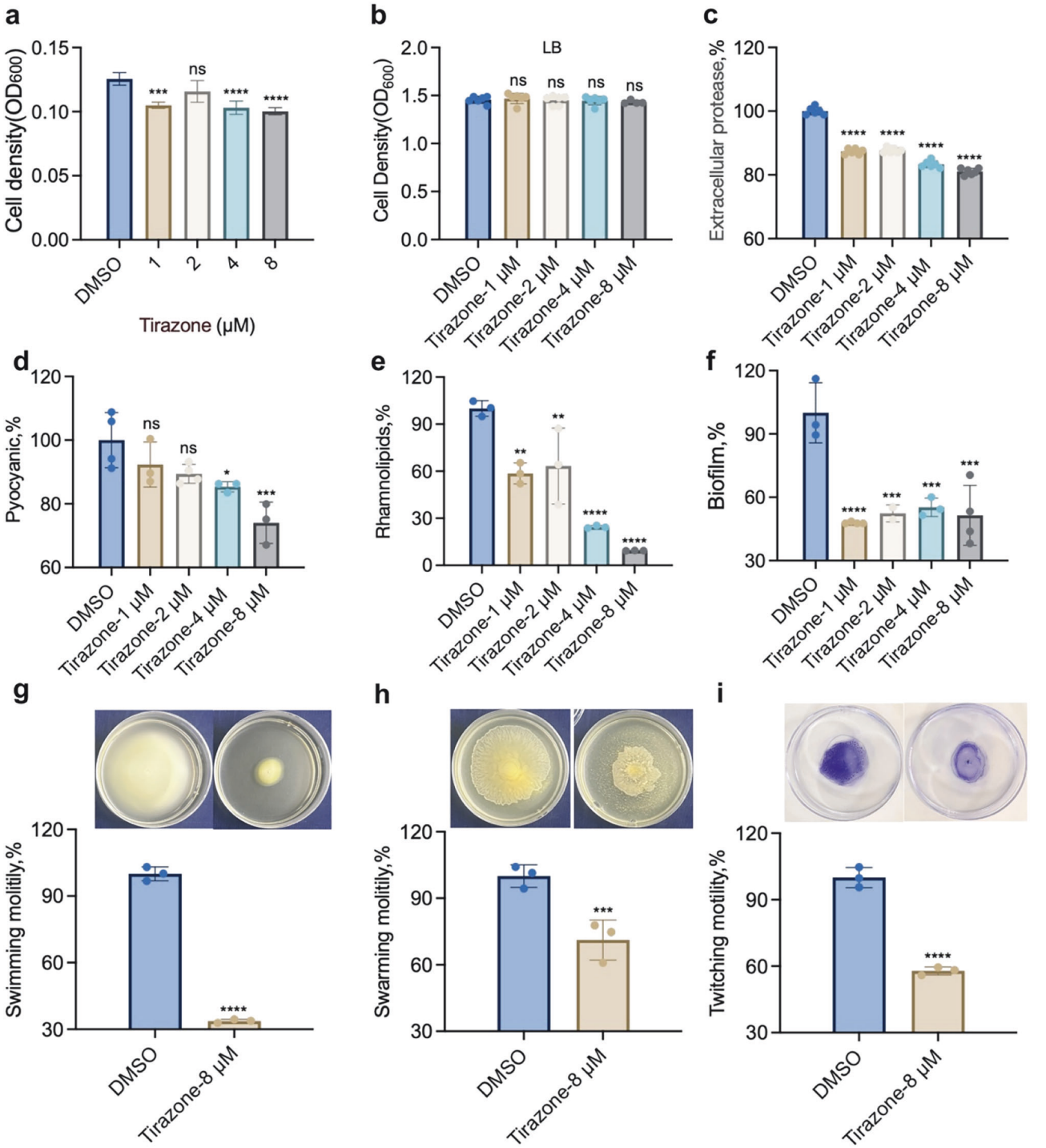

Fig. 2 Effect of Tirazone on *P. aeruginosa* PAO1 growth and Tirazone inhibits the virulence-related phenotypes of *P. aeruginosa* PAO1. **a** The growth curves of PAO1 in M9-adenosine (0.1%, w/v) medium containing different concentrations of Tirazone and cultured for 36 h at 37 °C. **b** The growth of PAO1 in LB medium containing different concentrations of Tirazone and cultured for 24 h at 37 °C. **c** Percentage of protease production of PAO1 in LB medium containing different concentrations of Tirazone. **d** Percentage of pyocyanin production of PAO1 in LB medium containing different concentrations of Tirazone. **e** Percentage of rhamnolipids production of PAO1 in LB medium containing different concentrations of Tirazone. **f** Percentage of biofilm formation of PAO1 in LB medium containing different concentrations of Tirazone.The effects of Tirazone (8 μM) on motility of PAO1 (**g**–**i**). **g** Swimming motility. **h** Swarming motility. **i** Twitching motility. Data shown are means ± SD of three independent experiments. The analysis methods were used one-way ANOVA or Student's *t* test, ns not significant, *, $P < 0.05$, **, $P < 0.01$, ***, $P < 0.001$, ****, $P < 0.0001$

(Fig. 2c, Table S3). Furthermore, phenotypic characterization demonstrated Tirazone's broad antivirulence activity, with concomitant suppression of pyocyanin biosynthesis (Fig. 2d) and rhamnolipid production (Fig. 2e). These results indicated that Tirazone exhibited a more comprehensive virulence regulation capability than the other tested compounds and was therefore identified as a candidate compound based on the results of phenotypic identification above.

Tirazone inhibited the biofilm formation of *P. aeruginosa*

Biofilms are structured aggregates formed by microorganisms. Their characteristic extracellular matrix (EPS) is composed of polysaccharides, proteins, and nucleic acids, which play a critical role in pathogen colonization and drug resistance [36]. QS systems not only regulate virulence factor expression but also mediate biofilm dynamics through multi-level regulatory networks. The results showed that biofilm formation of *P. aeruginosa* PAO1 was significantly inhibited in Tirazone-treated groups (Fig. 2f). Similarly, Tirazone also showed inhibition of biofilm formation of *P. aeruginosa* clinical isolates (Fig. S6c). These results suggested the effective activity of Tirazone in inhibiting the biofilm formation of *P. aeruginosa*.

Tirazone inhibits the motility of *P. aeruginosa*

The motility system serves as a crucial virulence factor for numerous pathogens, facilitating bacterial proliferation, colonization, and infection by allowing adaptation to diverse environmental conditions [37]. We then investigated the inhibitory effect of Tirazone on the motility of *P. aeruginosa*. Compared with the control group, Tirazone at the concentration of 8 μM significantly reduced the swimming, swarming, and twitching motilities of *P. aeruginosa* PAO1 by 67%, 25%, and 40%, respectively (Fig. 2g–i), with the most notable effect detected on the swimming motility. Moreover, the inhibitory effect of Tirazone on the cell motilities of *P. aeruginosa* was verified by using PA14 and other clinical isolates (Fig. S7).

Tirazone competitively inhibits the three QS pathways of *P. aeruginosa*

We then explored the molecular mechanism underlying the binding interaction between Tirazone and QS pathways by using the 3-oxo-C12-HSL-deficient strain PAO1-Δ*lasI*, C4-HSL-deficient strain PAO1-Δ*rhlI*, and PQS-deficient strain PAO1-Δ*pqsA*. RT-qPCR was used to detect the expression levels of corresponding virulence genes (*lasB*, *rhlA*, *phzA1*) regulated by the three QS pathways. The results showed that the addition of exogenous 3-oxo-C12-HSL at the concentration of 50 μM signficanly up-regulated *lasB* expression in PAO1-Δ*lasI* by 2.5-fold, while the co-treatment group (3-oxo-C12-HSL + 8 μM Tirazone) significantly inhibited *lasB* expression level (Fig. 3a). Similarly, the addition of 50 μM of C4-HSL induced a 4-fold increase in *rhlA* expression in PAO1-Δ*rhlI*, whereas *rhlA* expression was significantly decreased in the Tirazone and C4-HSL co-treatment group (Fig. 3b). Moreover, the addition of 8 μM of PQS could increase the expression level of *phzA1* in PQS-deficient strain PAO1-Δ*pqsA* by more than 5 times, while *phzA1* expression was suppressed upon the intervention of Tirazone (Fig. 3c). Subsequently, we also assessed the expression of QS-related virulence genes and identified a consistent downregulation trend in the Tirazone-treated group (Fig. 3d). Critically, we further validated the role of Tirazon by using clinically isolated strains and found that, compared to the remarkably suppressed bacterial growth in M9-adenosine medium and pyocyanin production by Tirazone, the supplementation of QS signals could partially restored these phenotypes (Fig. 4). These experiments confirmed that Tirazone competed with QS signal molecules to bind with the core regulatory proteins to regulate downstream virulence.

Synergistic effect of Tirazone with antibiotics on *P. aeruginosa*

We assessed the potential synergistic impact of Tirazone in combination with widely used clinical antibiotics. The MICs of levofloxacin, amikacin, and polymyxin B against *P. aeruginosa* PAO1 and clinical isolates were determined (Table S4). Subsequently, we evaluated the growth of *P. aeruginosa* when the antibiotics were administered individually or in conjunction with varying concentrations of Tirazone. The results showed that the addition of Tirazone could reduce the growth pressure of clinical bacteria brought by antibiotics. Tirazone in combination with levofloxacin significantly enhanced PAO1 sensitivity to this antibiotic (Fig. 5a, b). For levofloxacin-resistant clinical isolate 3-R5-1, the addition of 8 μM Tirazone reduced the MIC value from 5.4 μg/mL to 4.8 μg/mL over a concentration gradient of 0-6.6 μg/mL (Fig. 5c, d). In combination with amikacin, 4 μM Tirazone completely inhibited PAO1 growth at concentrations ranging from 0 to 0.33 μg/mL and exhibited significant synergistic antimicrobial effects at concentrations ranging from 0.12 to 0.21 μg/mL (Fig. 5e, f); this synergistic effect was concentration-dependent for amikacin-resistant clinical isolates (Fig. 5g, h). In addition, Tirazone in combination with polymyxin B presented synergistic antimicrobial activity against PAO1 (Fig. 5i, j) and clinical isolates (Fig. 5k, l). These results indicated that the combined use of Tirazone could

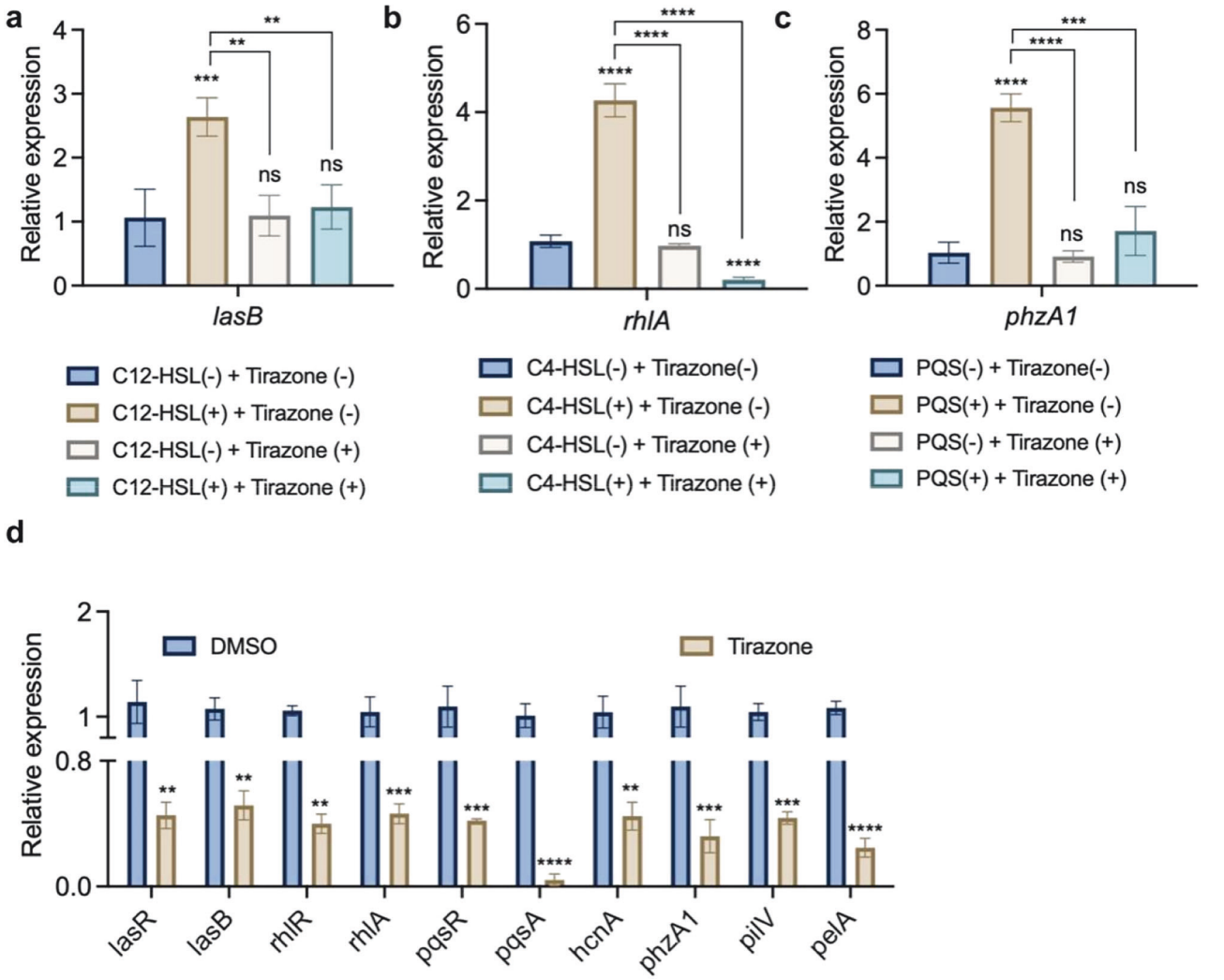

Fig. 3 The mechanism of anti-QS activity of Tirazone. **a** The expression of *lasB* in PAO1-Δ*lasI* under different conditions. **b** The expression of *rhlA* in PAO1-Δ*rhlA* under different conditions. **c** The expression of *phzA1* in PAO1-Δ*pqsA* under different conditions. **d** Expression of important QS genes of Tirazone-treated PAO1 was determined by RT-qPCR. Data shown are means ± SD of three independent experiments. The DMSO group values represent the actual relative expression levels (not normalized to 1) to reflect biological variability. Statistical significance was determined by one-way ANOVA or Student's *t*-test, ns not significant, *, $P < 0.05$, **, $P < 0.01$, ***, $P < 0.001$, ****, $P < 0.0001$

effectively enhance the efficiency of the antibiotics tested in this study against *P. aeruginosa* PAO1 and drug-resistant clinical strains.

Tirazone protects *C. elegans* and mice from *P. aeruginosa* infection

P. aeruginosa can cause acute infection and subsequent persistent infection by secreting a variety of virulence factors involved in host immune response and lung tissue damage [38]. We then investigated the in vivo protection activity of Tirazone against *P. aeruginosa* infection by using *C. elegans* and mouse models [39]. The results showed that Tirazone reduced the mortality of *C. elegans* against *P. aeruginosa* PAO1 infection, which mimics the acute infection conditions in the fast-kill assay (Fig. 6a), while not significantly ($P = 0.0520$). To further assess the protection of Tirazone, we also chose the highly virulent model strain PA14 to construct the infection model (Fig. 6b). As a result, Tirazone significantly increased the survival rate of *C. elegans* against *P. aeruginosa* PA14 infection ($P = 0.0057$). The above results indicated that Tirazone could effectively rescue *C. elegans* from *P. aeruginosa* challenge. Subsequently, we verified that Tirazone monotherapy significantly increased the survival rate ($P = 0.0034$) of *P. aeruginosa*-infected mice by establishing a mouse model of acute infection (Fig. 6c), and the survival rate was further increased in combination with polymyxin B ($P = 0.0084$) compared with the 2 × MIC polymyxin B monotherapy group ($P = 0.0420$).

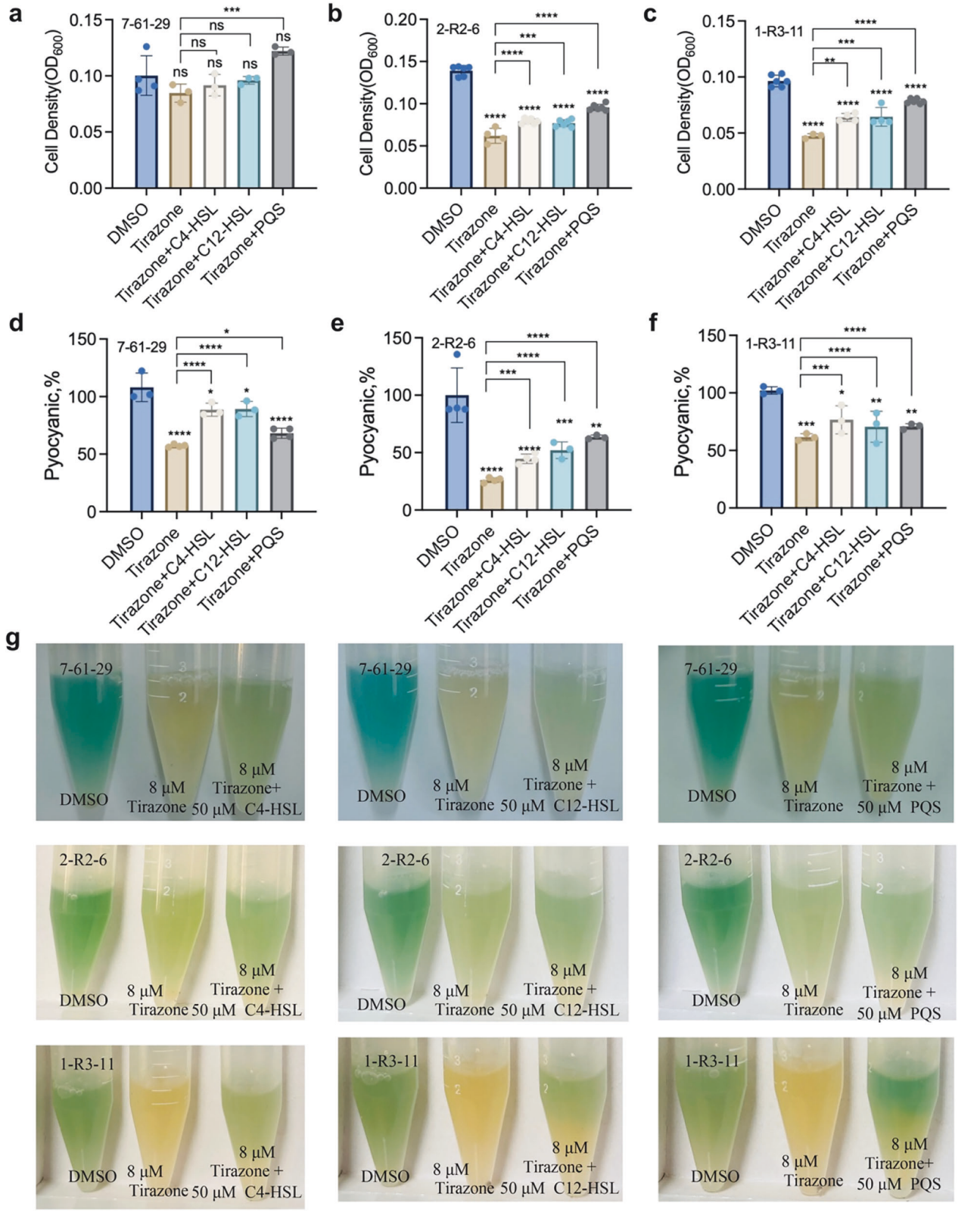

Fig. 4 Effects of Tirazone on clinical isolates. The growth of clinical isolates in M9-adenosine (0.1%, w/v) medium containing Tirazone (8 μM) (**a**–**c**). The pyocyanin production of clinical isolates in LB medium containing Tirazone supplementation with AIs (**d**–**f**). **h** The image of pyocyanin production of clinical isolates containing Tirazone supplementation with AIs. Data shown are means ± SD of three independent experiments. The analysis methods were used one-way ANOVA or t test, ns not significant, *, $P < 0.05$, **, $P < 0.01$, ***, $P < 0.001$, ****, $P < 0.0001$

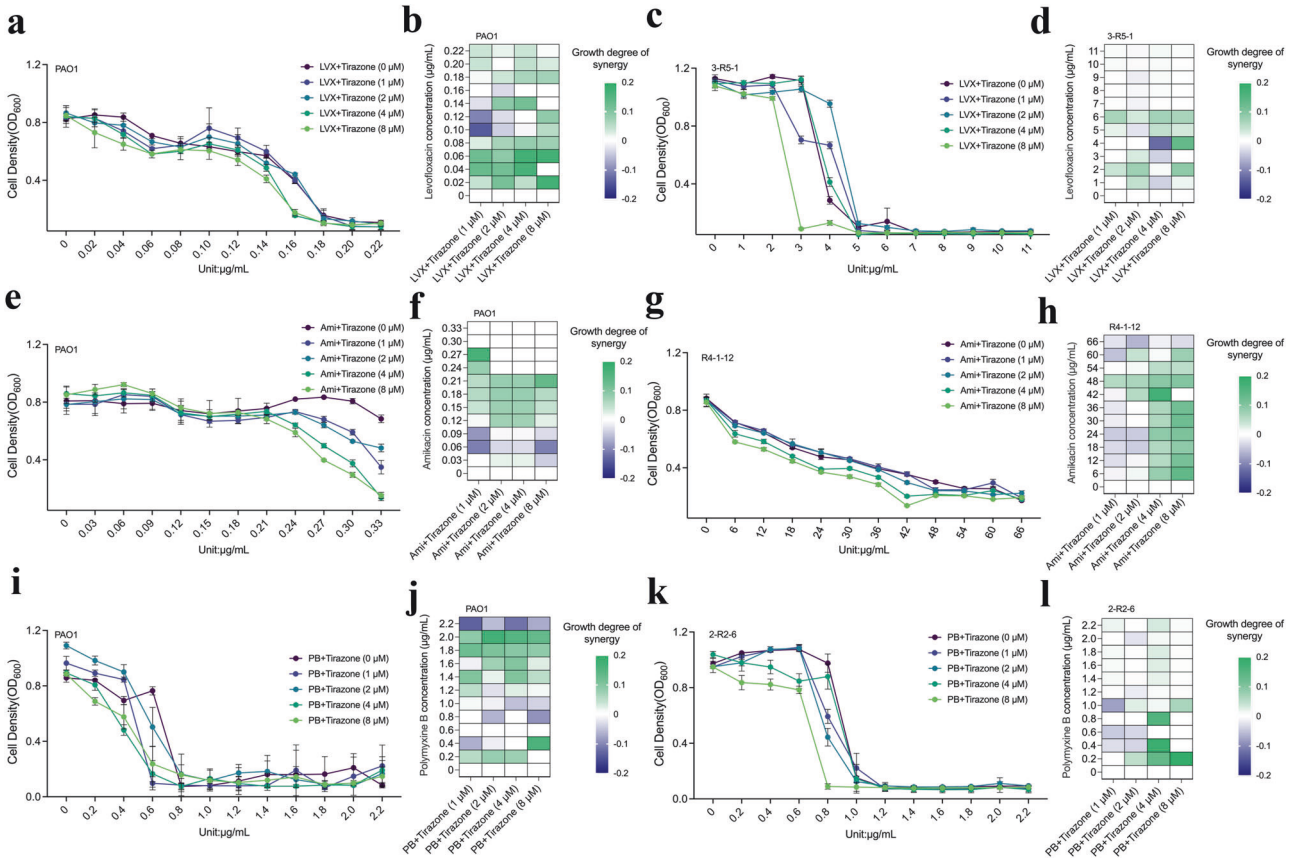

Fig. 5 The synergic interactions of Tirazone with antibiotics. **a** Growth curve of Tirazone combined with levofloxacin against PAO1 and the (**b**) Heap map. **c** Growth curve of Tirazone combined with levofloxacin against clinical isolate *P. aeruginosa* 3-R5-1 and the (**d**) Heap map. **e** Growth curve of Tirazone combined with amikacin against PAO1 and the (**f**) Heap map. **g** Growth curve of Tirazone combined with amikacin against clinical isolate *P. aeruginosa* R4-1-12 and the (**h**) Heap map. **i** Growth curve of Tirazone combined with polymyxin B against PAO1 and the (**j**) Heap map. **k** Growth curve of Tirazone combined with polymyxin B against clinical isolate *P. aeruginosa* 2-R2-6 and the (**l**) Heap map

Additionally, the mice of Tirazone monotherapy group exhibited significantly lower levels of residual *P. aeruginosa* in the lung bacterial load compared to the untreated group ($P < 0.0001$, Fig. 6d), while the combination group demonstrated enhanced efficacy ($P < 0.0001$). Pathological examinations indicated that the lung tissues of the untreated group and the group treated with 1/2 × MIC polymyxin B displayed degeneration and necrosis of alveolar epithelial cells with severe inflammatory infiltration. By contrast, the lungs of Tirazone-treated group and 2× MIC polymyxin B-treated group exhibited lesions to a lesser extent than the untreated group and the 1/2×MIC polymyxin B group. Moreover, the lung tissues of the Tirazone and 1/2× MIC polymyxin B co-treated group remained structurally intact, with significantly reduced inflammatory infiltration, closely resembling the normal physiological state (Fig. 6e). These results confirmed that Tirazone possesses not only anti-infective properties but also synergistically mitigates lung tissue damage induced by *P. aeruginosa* infection when combined with polymyxin B.

Safety profile and clinical feasibility of Tirazone for repurposing

A critical prerequisite for drug repurposing is the validation of a favorable safety profile and the feasibility of achieving effective concentrations in clinical settings. For Tirazone, Phase I-III clinical trials for its original antitumor indication [40, 41] have provided robust data on its human toxicity and pharmacokinetics. Dose-limiting toxicities (DLTs) of Tirazone, including ototoxicity and muscle cramps, are reversible and only observed at intravenous doses ≥330 mg/m², which are significantly higher than the concentrations required for QS inhibition (8 μM) in our study. Notably, Tirazone lacks myelosuppressive effects—a key advantage for combination therapy with anti-pseudomonal antibiotics (e.g., polymyxin B, levofloxacin), which often induce hematologic toxicity. Clinical trials further confirmed no treatment-related deaths at therapeutic doses, with adverse events resolving completely after drug discontinuation [40, 41]. The feasibility of achieving effective

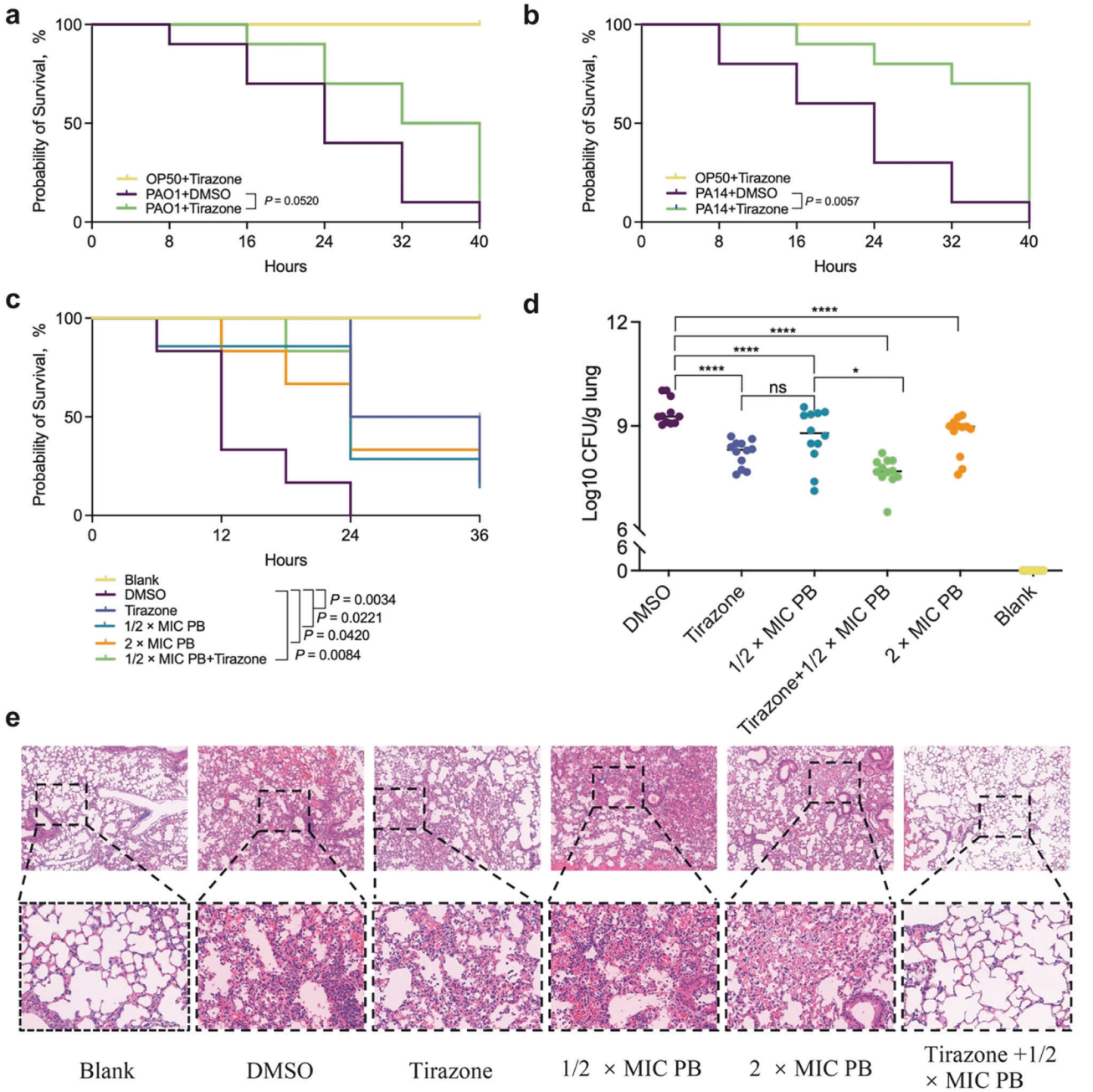

Fig. 6 Tirazone effectively protects the host from *P. aeruginosa* infection. **a** Protection of Tirazone (8 μM) on *C. elegans* models (10 nematodes per group) infected with *P. aeruginosa* PAO1 in the fast killing assay. **b** Protection of Tirazone (8 μM) on *C. elegans* models (10 nematodes per group) infected with *P. aeruginosa* PA14 in the fast killing assay. **c** Protection of Tirazone (8 μM) on mouse models (6 mice per group) intranasally instilled with *P. aeruginosa* PAO1. **d** Bacterial load at lung focus in mouse model of acute infection (12 mice per group). **e** Pathological sections of lung lesions in mice model of acute infection. The Mantel-Cox log-rank test was used for survival analysis. Bacterial colony-forming unit (CFU) counts were log10-transformed prior to one-way ANOVA to satisfy the assumption of normality. Data shown are means ± SD of three independent experiments. The analysis methods were used one-way ANOVA, ns not significant, *, $P < 0.05$, **, $P < 0.01$, ***, $P < 0.001$, ****, $P < 0.0001$

concentrations while minimizing systemic risk is enhanced by our proposed local administration route (e.g., inhalation for pulmonary infections). Intravenous administration of Tirazone at 330 mg/m² achieves transient peak plasma concentrations of ~ 5.8–7.9 μM [41], which is close to the 8 μM effective concentration in our study. However, local delivery directly targets the infection site (e.g., lung epithelium for pulmonary infections) to maintain sustained effective concentrations, while drastically reducing systemic drug exposure—thus avoiding DLTs associated with high

intravenous doses. Preclinical studies further support Tirazone's low host toxicity. In tumor-bearing mouse models, Tirazone monotherapy induced only minimal and transient weight loss (<7%) without significant pathological damage to vital organs (liver, kidney, heart) [42, 43]. In our *P. aeruginosa* infection models, Tirazone monotherapy did not exacerbate host injury but instead reduced infection-related pathology (Fig. 6e), confirming that it does not add appreciable toxicity in the context of infection. Collectively, these data demonstrate that Tirazone's safety profile, combined with the feasibility of local administration, supports its repurposing as a safe and effective adjunctive therapy for *P. aeruginosa* infections.

Discussion

Antibiotic resistance in bacteria has escalated into a critical global public health crisis. According to the latest statistics, approximately 1.27 million people die directly from drug-resistant infections each year [3], and this number is projected to soar to 10 million annually by 2050 [44]. The World Health Organization (WHO) has classified ESKAPE pathogens (*Enterococcus faecalis*, *Staphylococcus aureus*, *Klebsiella pneumoniae*, *Acinetobacter baumannii*, *P. aeruginosa*, and *Enterobacter species*) as priority pathogens due to their evolving resistance to multiple antibiotics and associated high mortality rates [45]. As a typical multidrug-resistant opportunistic pathogen, *P. aeruginosa* poses a life-threatening risk to immunocompromised patients through rapid evolutionary adaptations [46].

While novel antimicrobial agents such as next-generation β-lactamase inhibitors continue to be developed, the accelerated evolution of drug-resistant strains has severely compromised the clinical efficacy of existing therapies [2]. Meanwhile, the development of new antibiotics faces a dual dilemma: on the one hand, drug development cycles typically exceed a decade; on the other hand, the number of clinically viable candidate molecules continues to decline [47]. Against this backdrop, innovative therapeutic strategies for *P. aeruginosa* infections are urgently needed. Drug repurposing has emerged as a promising approach, with successful applications of non-antimicrobial agents such as flucytosine (inhibits the expression of the iron-deficiency sigma factor PvdS), sitagliptin (targets QS signaling pathways), and cisplatin (regulates the Type III secretion system, T3SS)—all benefiting from short development cycles and cost-effectiveness [48–50].

The pathogenicity of *P. aeruginosa* is governed by a hierarchical regulatory network consisting of three QS systems: Las, Rhl, and Pqs [12]. The Las system occupies the apex of this regulation, with its core protein LasR controlling the expression of the Rhl and Pqs systems through cascading effects, making LasR a primary target for traditional QS inhibitors [51]. However, clinical studies have found that LasR mutants account for over 30% of isolates from patients with chronic lung infections [52], posing significant challenges to LasR-targeted therapeutic strategies. Although the Rhl system is regulated by the Las system, its core protein RhlR directly participates in the regulation of virulence factor expression; knocking out either the lasR or rhlR gene alone neither completely blocks QS responses nor significantly attenuates bacterial virulence [53]. The regulatory mechanism of the Pqs system is more complex: its synthesis depends on the *pqsABCDE* operon activated by PqsR, where *pqsABCD* are essential genes for PQS signal molecule synthesis. In contrast, *pqsE*, while not involved in PQS synthesis, can directly activate virulence-related genes independently of PQS/PqsR, serving as a key escape pathway to evade inhibitor action [54]. Furthermore, this bacterium employs hierarchical redundancy (compensatory functions of Rhl/Pqs for Las), functional escape (*pqsE*-independent activation), and multi-virulence factor synergy to render single-target inhibitors ineffective. Based on these insights, this study aimed to develop multi-target QS inhibitors that simultaneously target the Las, Rhl, and Pqs systems to disrupt their QS regulatory network.

Molecular docking analysis confirmed that Tirazone not only localizes to the canonical ligand-binding pocket of LasR but also simultaneously binds to two other key QS receptors in *P. aeruginosa*, RhlR and PqsR. Although its calculated binding free energy for LasR (–5.48 kcal/mol) was slightly higher than that of its native autoinducer 3-oxo-C12-HSL (–6.26 kcal/mol) (Fig. 1h), with a similar trend observed for RhlR and PqsR, detailed analysis of molecular interactions revealed a significantly optimized binding mode—including the formation of a stable salt-bridge network with LasR residues Phe-101/Ala-105, strong hydrophobic interactions with the Ala-111/Phe-101 domain of RhlR, and multiple interactions with PqsR residues Gln194, Arg209, Leu207, and Ile203 (Fig. 1e–g)—which combined with functional rescue experiments (where 50 μM 3-oxo-C12-HSL reversed the inhibitory effect), confirms a competitive inhibition mechanism. The potent functional inhibition exhibited by Tirazone despite its somewhat weaker thermodynamic affinity can be rationally explained by effective local concentration and binding kinetics (e.g., dissociation rate and target residence time): Tirazone was applied at 8 μM in experimental systems, a concentration far exceeding the nanomolar physiological level of native QS signals in *P. aeruginosa* under basal conditions, creating a local concentration advantage that facilitates competitive occupation of receptor-binding sites in line with the "concentration threshold effect" observed in QSI research [55]; consistent with the well-established principle that drug-target residence time ($\tau = 1/koff$) often exerts a more critical

impact on efficacy than equilibrium binding affinity [56], Tirazone's optimized binding mode—featuring stable salt bridges and hydrophobic interactions with target receptors—likely confers a slower dissociation rate relative to native ligands, as similar interaction patterns in QS inhibitors have been shown to prolong target occupancy [56]; meanwhile, molecular dynamics simulations further demonstrate that Tirazone induces conformational changes in LasR (e.g., stabilizing the salt bridge between His264 and Glu169) through an induced-fit mechanism, enhancing binding stability and blocking native ligand-binding channels, which aligns with the notion that receptor conformational flexibility modulates inhibitor activity [56, 57]. This phenomenon of "weak thermodynamic affinity but potent functional inhibition" is prevalent in QSI research—for example, halogenated furanones achieve competitive inhibition of *P. aeruginosa* QS systems through similar concentration advantages and kinetic characteristics despite lower binding affinity than native signal molecules [58]—and such discrepancies between functional efficacy and thermodynamic data arise from the synergistic effects of thermodynamic affinity, kinetic parameters, local concentration, and receptor conformational dynamics in the dynamic non-equilibrium in vivo environment, rather than reliance on equilibrium binding free energy alone [59], Aligning with the modern drug discovery principle that efficacy depends not merely on thermodynamic affinity but critically on kinetic behavior and effective site occupancy [55, 56, 60], Tirazone's unique multi-target binding conformation provides a structural basis for its functional efficacy and may confer advantageous properties compared to some classical QS inhibitors [17, 28, 29].

Experimental validation demonstrated that Tirazone significantly inhibits virulence factor secretion, bacterial motility, and biofilm formation in *P. aeruginosa* (Fig. 2c–i). Its mechanism of action involves the multi-target regulation of the QS system by competing with the natural small molecules of QS for binding to target proteins, thereby interfering with QS signal transduction (Fig. 3a–c). Notably, Tirazone also exhibited consistent efficacy against clinical isolates, effectively inhibiting biofilm formation and bacterial motility (Fig. S7), highlighting its effectiveness against clinically relevant strains beyond laboratory models. A study has confirmed that Tirazone can downregulate the expression of QS-related proteins in *E. coli* [61]. In contrast, the present study focuses on the complex Las/Rhl/Pqs QS system of *P. aeruginosa*. Importantly, compared to its regulatory mechanism targeting the AI-2 signaling pathway in *E. coli*, Tirazone's inhibitory effect on the *P. aeruginosa* QS system exhibits species-specific differences, reflecting the evolutionary diversity of QS networks among different bacteria and the strain-specific mechanism of Tirazone's action. Further in vivo experiments demonstrated that Tirazone provides significant protection against infection by the highly virulent PA14 strain in a *C. elegans* acute infection model; in a mouse model of *P. aeruginosa* infection, Tirazone improved survival rates, reduced lung bacterial loads, and alleviated pulmonary pathological damage (Fig. 6). Importantly, Tirazone demonstrated significant synergistic effects with several clinically relevant antibiotics (levofloxacin, amikacin, and polymyxin B) against both the laboratory reference strain PAO1 and drug-resistant clinical isolates, suggesting a promising role in combination therapy (Fig. 5). Crucially, a favorable safety profile for Tirazone has been established through Phase I-III clinical trials for its original antitumor indication, providing significant support for its repurposing: dose-limiting toxicities (ototoxicity, muscle cramps) are reversible and only occur at intravenous doses ≥330 mg/m² [40, 41], while the local administration routes (e.g., inhalation) proposed for antimicrobial use in this study can minimize systemic exposure and further reduce toxicity risks. This favorable safety profile, combined with its demonstrated in vivo efficacy, lays a critical foundation for clinical translation.

Based on the inherent regulatory crosstalk between the QS system and efflux pumps in *P. aeruginosa*, as well as the confirmed QS inhibitory activity of Tirazone, we propose a mechanistic hypothesis to explain its synergistic effects. The synergistic efficacy observed between Tirazone and antibiotics in both PAO1 and clinical strains may stem from Tirazone's multi-target inhibition of the QS system, thereby broadly attenuating the bacterial adaptive resistance response. Tirazone likely attenuates bacterial drug resistance and enhances antibiotic efficacy by targeting the Las/Rhl/Pqs QS system through multiple interconnected pathways. This multi-faceted suppression of QS signaling may lead to the downregulation of key efflux pump systems and other resistance determinants that are normally activated during stress, ultimately restoring or enhancing antibiotic susceptibility. For instance, it may inhibit the synthesis of QS signaling molecules and indirectly downregulate the transcription of core efflux pump genes—for levofloxacin, this may involve reducing the expression of *MexAB-OprM* and *MexCD-OprJ* [62–64]; for amikacin, it may decrease *MexXY-OprM* expression [62, 65, 66]; for polymyxin B, it may suppress the Pqs system to downregulate *MexEF-OprN* and lipopolysaccharide-modifying enzymes [67, 68]. This hypothesis is consistent with the established mode of action of QS inhibitors in enhancing antibiotic sensitivity by regulating efflux pump expression [62, 69].

In summary, this study delineates the multifaceted antivirulence activity of Tirazone against *P. aeruginosa*. Its demonstrated ability to potentiate antibiotic effects across diverse strains underscores its potential as a resistance-modifying agent. These findings not only highlight Tirazone's potential as an antivirulence drug but also provide a

theoretical basis for the development of "antivirulence-antibacterial" synergistic therapeutic strategies for the clinical management of *P. aeruginosa* infections.

Data availability

The datasets supporting the findings of this study are publicly available in the Figshare repository and can be accessed via the permanent https://doi.org/10.6084/m9.figshare.29301779.

Acknowledgements We sincerely thank Prof. Xikun Zhou from Sichuan University for his kind help in coordinating the animal experiments of this study.

Author contributions KZ and LDu conceptualized and led the project. MF, XH, YW, SG, QR and YY performed the experiments. XW, L Dan, YC, XZ, and TH facilitated the procurement of essential materials and equipment. MF and XW analyzed the data, interpreted the results, and drafted the thesis. KZ and L Du reviewed and revised the manuscript in its entirety and provided final approval for publication. All authors have reviewed the final manuscript and consented to assume responsibility for all aspects of the research.

Funding This work was supported by the National Natural Science Foundation of China (32270121 to KZ, 32200525 to L Du and 32400477 to L Dan), the Natural Science Foundation of Sichuan Province (2023NSFSC1231 to L Dan) and the High-level Talent Training Program of Chengdu University (2081920066 to KZ).

Compliance with ethical standards

Conflict of interest The authors declare no competing interests.

References

1. Hutchings MI, Truman AW, Wilkinson B. Antibiotics: past, present and future. Curr Opin Microbiol. 2019;51:72–80.
2. Oliveira M, et al. An overview of the recent advances in antimicrobial resistance. Microorganisms. 2024;12:1920.
3. Naghavi M, et al. Global burden of bacterial antimicrobial resistance 1990–2021: a systematic analysis with forecasts to 2050. Lancet. 2024;404:1199–226.
4. Muteeb G, Rehman MT, Shahwan M, Aatif M. Origin of antibiotics and antibiotic resistance, and their impacts on drug development: a narrative review. Pharmaceuticals. 2023;16:1615.
5. Li J, Jia T, Yang L. Targeting anti-virulence factor strategies of bacterial pathogens. Biosaf Health. 2025;7:1–4.
6. Xiao Y, et al. Impact of quorum-sensing signaling molecules in Gram-negative bacteria on host cells: current understanding and future perspectives. Gut Microbes. 2022;14:2039048.
7. Azimi S, Klementiev AD, Whiteley M, Diggle SP. Bacterial quorum sensing during infection. Annu Rev Microbiol. 2020;74:201–19.
8. Inoue Y, Togashi N, Hamashima H. Farnesol-induced disruption of the *Staphylococcus aureus* cytoplasmic membrane. Biol Pharm Bull. 2016;39:653–6.
9. Naga NG, Shaaban MI, El-Metwally MM. An insight on the powerful of bacterial quorum sensing inhibition. Eur J Clin Microbiol Infect Dis. 2024;43:2071–81.
10. Qin S, et al. *Pseudomonas aeruginosa*: pathogenesis, virulence factors, antibiotic resistance, interaction with host, technology advances and emerging therapeutics. Sig Transduct Target Ther. 2022;7:199.
11. Chadha J, Harjai K, Chhibber S. Revisiting the virulence hallmarks of *Pseudomonas aeruginosa*: a chronicle through the perspective of quorum sensing. Environ Microbiol. 2022;24:2630–56.
12. Lee J, Zhang L. The hierarchy quorum-sensing network in *Pseudomonas aeruginosa*. Protein Cell. 2015;6:26–41.
13. Nadal Jimenez P, et al. The multiple signaling systems regulating virulence in *Pseudomonas aeruginosa*. Microbiol Mol Biol Rev. 2012;76:46–65.
14. Rutherford ST, Bassler BL. Bacterial quorum sensing: its role in virulence and possibilities for its control. Cold Spring Harb Perspect Med. 2012;2:a012427.
15. Papenfort K, Bassler BL. Quorum-sensing signal–response systems in Gram-negative bacteria. Nat Rev Microbiol. 2016;14:576–88.
16. Zhao K. *Pseudomonas aeruginosa* quorum-sensing and type VI secretion system can direct interspecific coexistence during evolution. Front Microbiol. 2018;9:2287.
17. Yuan Y, et al. Repurposing dimetridazole and ribavirin to disarm *Pseudomonas aeruginosa* virulence by targeting the quorum-sensing system. Front Microbiol. 2022;13:978502.
18. Krishnan T, Yin W-F, Chan K-G. Inhibition of quorum-sensing-controlled virulence factor production in *Pseudomonas aeruginosa* PAO1 by ayurveda spice clove (Syzygium Aromaticum) bud extract. Sensors. 2012;12:4016–30.
19. Du L, et al. Dockey: a modern integrated tool for large-scale molecular docking and virtual screening. Brief Bioinform. 2023;24:bbad047.
20. Wiegand I, Hilpert K, Hancock REW. Agar and broth dilution methods to determine the minimal inhibitory concentration (MIC) of antimicrobial substances. Nat Protoc. 2008;3:163–75.
21. Toussaint, J-P et al. Gene duplication in *Pseudomonas aeruginosa* improves growth on adenosine. J Bacteriol 2017;199:e00261–17.
22. Zhao K, et al. Genetic and functional diversity of *Pseudomonas aeruginosa* in patients with chronic obstructive pulmonary disease. Front Microbiol. 2020;11:598478.
23. Das T, Manefield M. Pyocyanin promotes extracellular DNA release in *Pseudomonas aeruginosa*. PLoS ONE. 2012;7:e46718.
24. Wang S, et al. Inhibition of virulence factors and biofilm formation by wogonin attenuates pathogenicity of *Pseudomonas aeruginosa* PAO1 via targeting pqs quorum-sensing system. Int J Mol Sci. 2021;22:12699.
25. Shukla, SK, Rao, TS. An improved crystal violet assay for biofilm quantification in 96-well microtitre plate. 2017 Preprint at https://doi.org/10.1101/100214.
26. Pfeifer V, Beier S, Alirezaeizanjani Z, Beta C. Role of the two flagellar stators in swimming motility of *Pseudomonas putida*. mBio. 2022;13:e02182–22.
27. Ha D–G, Kuchma, SL, O'Toole, GA. Plate-Based Assay for Swarming Motility. In: Filloux A, & Ramos J-L, editors. Pseudomonas aeruginosa: Methods and Protocols. New York: Springer-Verlag; 2014. p. 67–72.
28. Wen F, et al. Discovery of psoralen as a quorum-sensing inhibitor suppresses *Pseudomonas aeruginosa* virulence. Appl Microbiol Biotechnol. 2024;108:222.
29. Wu Y, et al. Multifaceted quorum-sensing inhibiting activity of 3-(Benzo[d] [1,3] dioxol-4-yl) oxazolidin-2-one mitigates *Pseudomonas aeruginosa* virulence. Virulence. 2025;16:2479103.
30. Huang T, et al. A potent antibiotic combination of linezolid and polymycin B nonapeptide against *Klebsiella pneumoniae* infection in vitro and in vivo. Front Pharmacol. 2022;13:887941.
31. Liu Q, Yin X, Languino LR, Altieri DC. Evaluation of drug combination effect using a Bliss independence dose–response surface model. Stat Biopharm Res. 2018;10:112–22.

32. Desalermos A, Muhammed M, Glavis-Bloom J, Mylonakis E. Using *Caenorhabditis elegans* for antimicrobial drug discovery. Expert Opin Drug Discov. 2011;6:645–52.
33. Mazzolini R, et al. Engineered live bacteria suppress *Pseudomonas aeruginosa* infection in mouse lung and dissolve endotracheal-tube biofilms. Nat Biotechnol. 2023;41:1089–98.
34. Muhlen, S, Dersch, P. Anti-virulence strategies to target bacterial infections. In: Stadler M, & Dersch P, editors. How to overcome the antibiotic crisis. Cham: Springer International Publishing; 2015. p. 147–83.
35. Alatraktchi FA, Svendsen WE, Molin S. Electrochemical detection of pyocyanin as a biomarker for *Pseudomonas aeruginosa*: a focused review. Sensors. 2020;20:5218.
36. Carradori S, et al. Biofilm and quorum-sensing inhibitors: the road so far. Expert Opin Ther Pat. 2020;30:917–30.
37. Martínez E, Campos-Gómez J. Oxylipins produced by *Pseudomonas aeruginosa* promote biofilm formation and virulence. Nat Commun. 2016;7:13823.
38. Sandri A, et al. Inhibition of *Pseudomonas aeruginosa* secreted virulence factors reduces lung inflammation in CF mice. Virulence. 2018;9:1008–18.
39. Conery AL, Larkins-Ford J, Ausubel FM, Kirienko NV. High-throughput screening for novel anti-infectives using a *C. elegans* pathogenesis model. CP Chem Biol. 2014;6:25–37.
40. Marcu L, Olver I. Tirapazamine: from bench to clinical trials. Curr Clin Pharmacol. 2006;1:71–9.
41. Gatzemeier U, et al. Tirapazamine-cisplatin: the synergy. Br J Cancer. 1998;77:15–7.
42. Adam M, et al. Tirapazamine plus cisplatin and irradiation in a mouse model: improved tumor control at the cost of increased toxicity. J Cancer Res Clin Oncol. 2007;134:137–46.
43. Adam M, et al. Untersuchungen zur Toxizität von Tirapazamin plus Cisplatin in einem Maus-Tumormodell. Strahlenther Onkol. 2006;182:231–9.
44. Okeke IN, et al. The scope of the antimicrobial resistance challenge. Lancet. 2024;403:2426–38.
45. Luo Q, et al. ESKAPE in China: epidemiology and characteristics of antibiotic resistance. Emerg Microbes Infect. 2024;13:2317915.
46. Monroy-Pérez E, et al. Molecular properties of virulence and antibiotic resistance of *Pseudomonas aeruginosa* causing clinically critical infections. Pathogens. 2024;13:868.
47. Hurley MN, Cámara M, Smyth AR. Novel approaches to the treatment of *Pseudomonas aeruginosa* infections in cystic fibrosis. Eur Respir J. 2012;40:1014–23.
48. Yuan M, et al. Repurposing the anticancer drug cisplatin with the aim of developing novel *Pseudomonas aeruginosa* infection control agents. Beilstein J Org Chem. 2018;14:3059–69.
49. Imperi F, et al. Repurposing the antimycotic drug flucytosine for suppression of *Pseudomonas aeruginosa* pathogenicity. Proc Natl Acad Sci USA. 2013;110:7458–63.
50. Hegazy WAH, et al. Repurposing anti-diabetic drugs to cripple quorum sensing in *Pseudomonas aeruginosa*. Microorganisms. 2020;8:1285.
51. Choi H-Y, Le DD, Kim W-G. Curvularin isolated from Phoma macrostoma is an antagonist of RhlR quorum sensing in *Pseudomonas aeruginosa*. Front Microbiol. 2022;13:913882.
52. Ding F, et al. Multidrug-resistant *Pseudomonas aeruginosa* is predisposed to lasR mutation through up-regulated activity of efflux pumps in non-cystic fibrosis bronchiectasis patients. Front Cell Infect Microbiol. 2022;12:934439.
53. Soto-Aceves MP, et al. Inactivation of the quorum-sensing transcriptional regulators LasR or RhlR does not suppress the expression of virulence factors and the virulence of *Pseudomonas aeruginosa* PAO1. Microbiology. 2019;165:425–32.
54. Deng J, et al. Isovanillin decreases the virulence regulated by the quorum-sensing system of *Pseudomonas aeruginosa*. Microb Pathog. 2024;196:107010.
55. Rasmussen TB, Givskov M. Quorum-sensing inhibitors as anti-pathogenic drugs. Int J Med Microbiol. 2006;296:149–61.
56. Pan AC, Borhani DW, Dror RO, Shaw DE. Molecular determinants of drug–receptor binding kinetics. Drug Discov Today. 2013;18:667–73.
57. Copeland RA. The drug–target residence time model: a 10-year retrospective. Nat Rev Drug Discov. 2016;15:87–95.
58. Segala E, et al. Controlling the dissociation of ligands from the adenosine A_{2A} receptor through modulation of salt bridge strength. J Med Chem. 2016;59:6470–9.
59. Zhou J-W, et al. Attenuation of *Pseudomonas aeruginosa* biofilm by hordenine: a combinatorial study with aminoglycoside antibiotics. Appl Microbiol Biotechnol. 2018;102:9745–58.
60. Babylon Education Directorate, Ministry of Education, Iraq et al. Kinetic and thermodynamic principles underlying drug–target interactions: a review article. Int J Med Sci Dent Health. 2025;11:66–70.
61. Wu Z, et al. New insights into the antimicrobial action and protective therapeutic effect of tirapazamine towards *Escherichia coli*-infected mice. Int J Antimicrob Agents. 2023;62:106923.
62. Chu X, Yang Q. Regulatory mechanisms and physiological impacts of quorum sensing in gram-negative bacteria. Infect Drug Resist. 2024;ume 17:5395–410.
63. Masuda N, et al. Substrate specificities of MexAB-OprM, MexCD-OprJ, and MexXY-OprM efflux pumps in *Pseudomonas aeruginosa*. Antimicrob Agents Chemother. 2000;44:3322–7.
64. Zahedi Bialvaei A, et al. Expression of RND efflux pumps mediated antibiotic resistance in *Pseudomonas aeruginosa* clinical strains. Microb Pathog. 2021;153:104789.
65. Singh M, Sykes EME, Li Y, Kumar A. MexXY RND pump of *Pseudomonas aeruginosa* PA7 effluxes bi-anionic β-lactams carbenicillin and sulbenicillin when it partners with the outer membrane factor OprA but not with OprM. Microbiology. 2020;166:1095–106.
66. Seupt A, Schniederjans M, Tomasch J, Häussler S. Expression of the MexXY aminoglycoside efflux pump and presence of an aminoglycoside-modifying enzyme in clinical *Pseudomonas aeruginosa* isolates are highly correlated. Antimicrob Agents Chemother. 2020;65:e01166–20.
67. Mlynarcik P, Kolar M. Molecular mechanisms of polymyxin resistance and detection of mcr genes. Biomed Pap Med Fac Univ Palacky Olomouc Czech Repub. 2019;163:28–38.
68. Lorusso AB, Carrara JA, Barroso CDN, Tuon FF, Faoro H. Role of efflux pumps on antimicrobial resistance in *Pseudomonas aeruginosa*. IJMS. 2022;23:15779.
69. Wang J, et al. Research progress on the combination of quorum-sensing inhibitors and antibiotics against bacterial resistance. Molecules. 2024;29:1674.